RGNZ/MGPB

Rudarsko-geološko-naftni zbornik
(The Mining-Geology-Petroleum Engineering Bulletin)
UDC: 622:333
DOI: 10.17794/rgn.2023.2.8

Preliminary communication

Assessment of Rock Slope Stability in a Humid Tropical Region: Case Study of a Coal Mine in South Kalimantan, Indonesia

Zulfahmi Zulfahmi[1*]; Dwi Sarah[2]; Franto Novico[3]; Robertus B. Susilo[4]

[1] *Research Center for Geological Resources, National Research and Innovation Agency, Bandung, West Java-Indonesia, 40135. ORCID https://orcid.org/0000-0002-7769-0391*

[2] *Research Center for Geological Disaster, National Research and Innovation Agency, Bandung, West Java-Indonesia, 40135. ORCID https://orcid.org/0000-0003-2707-3464*

[3] *Research Center for Geological Disaster, National Research and Innovation Agency, Bandung, West Java-Indonesia, 40135. ORCID https://orcid.org/0000-0001-6883-5029*

[4] *PT. Tanjung Alam Jaya, Banjarbaru, South Kalimantan – Indonesia, 70714*

Abstract

PT.X, a coal mining company in South Kalimantan, Indonesia, plans to use the highwall mining method to excavate marginal reserves on the final slope to maintain production. However, the stability of the slope and determination of the highwall mining dimensions are major concerns due to unfavourable rock mass conditions caused by intensive weathering and tectonics. This paper aims to evaluate the feasibility of highwall mining in the study area using empirical, analytical and numerical methods. The innovation of this research is the integration of these methods, which include rock mass classification, analytical calculation of load and rock support strength, 2D and 3D numerical modelling, and estimation of recovered coal from the highwall design. The initial condition assessment using rock mass classification and analytics calculation of the mining geometry model determined mine openings and pillar dimensions. Numerical modelling re-evaluated the geometry models to obtain an optimal design. The suggested optimal thickness, mine opening, web pillars, and barrier pillars are 3.20, 3.00, 3.50, and 4.00 m, respectively, with four web pillars in one panel at Seam-C and 2.50, 3.00, 3.50, and 4.00 m with four web pillars in one panel at Seam-D. The recovery of coal for Seam-C and Seam-D is estimated to be 40.54%. Deformation was found to have the closest relationship with the dimensions of the mine opening, and the safety factor is most sensitive to changes in the depth of the mine opening. This study provides a reference for future highwall mining in Indonesia and other regions with similar conditions.

Keywords:

Highwall mining; stability; empirical; analytical; numerical modelling

1. Introduction

Indonesia is one of the largest coal producers worldwide and ranks as the fifth largest producer and second most significant exporter **(Baskoro et al., 2021)**. Most of its coal reserves are mined from the surface by the open cut method (**Sasaoka et al., 2016**). One of them is PT.X, which is located in South Kalimantan. This company has five mining sites, with the fifth location almost reaching the pit limit with a high stripping ratio. They plan to continue mining at this fifth location using the underground method; however, further exploration still needs to ensure the continuity of the deep coal reserves. It takes a long time to get to the production stage. Moreover, there needs to be a method that can immediately continue to exploit the coal on the fifth site that has almost finally reached its economic limit due to the high stripping ratio to maintain coal production for domestic and export supply. As the surface to underground mine transitions, PT.X plans to extract coal seam at the final wall of the mine or highwall that still leaves valuable reserves.

The highwall mining method can recover the coal reserves on this final wall and can be developed with a fast time and return on investment. This method is suitable for small marginal coal reserves with a limited residual mining space or considered only for small areas where longwall mining is troublesome to apply (**Spearing, Zhang, and Ma, 2021**) or before the commencement of underground mining (**Shimada et al., 2013**). Some researchers even mention that highwall mining is a combined mining technology between surface and underground (**Kuznetsova and Anfyorov, 2019**) and as a prelude before underground mining is applied (**Seib, 1993; Sasaoka et al., 2015; Sasaoka et al., 2016**). Optimisation of marginal coal reserves using highwall mining is in line with the Ministry of Energy and Mineral

Corresponding author: Zulfahmi Zulfahmi
e-mail address: zulf009@brin.go.id

Resources of Indonesia Decree No. 1827 K/30/MEM/2018 on good mining practices stipulating utilising marginal reserves. One of the content articles is that every mining company must plan to utilise the residual resources after the primary mining activities have been carried out. Optimisation of residual reserve utilisation can be considered a concern for conserving mineral and coal reserves.

Highwall mining has become a new standard practice in open-cut mining in countries like China, Australia, India, and Russia to maximise coal recovery from marginal reserves (**Tian et al., 2023**). Highwall mining involves extracting coal from the base of the highwall using a series of parallel entries driven into the coal seam, typically using continuous highwall mining and auger mining (**Shen, 2014**). Compared to underground and open cut methods, highwall mining has advantages (**Mo et al., 2016**): (1) it is flexible and mobile due to the ease of extracting coal blocks from small and constrained areas, (2) it is economically competitive due to low operation costs and (3) it is a safe mining method because the operators are out of the mine entries. However, this method has some considerations, particularly on slope stability and subsidence issues.

The stability of highwall mining faces problems from the slopes, interlayer between openings, and pillars; the problems become more complex when dealing with multi-seams and steeply dipping coal seams (**Ross et al., 2019; Tian et al., 2023**). Comparable to room and pillar mining, the loss of support from the pillar can cause instability (i.e. subsidence) (**Sarfarazi et al., 2022**). To ensure a safe operation of highwall mining, the web pillar and rib pillar layout must be arranged to support the overall stability. **Sarfarazi et al. (2022)** and **Sarfarazi et al. (2023)** investigated the failure behaviour of room and pillar mining with different shapes and room configurations under uniaxial loading using experimental and numerical methods. **Sarfarazi et al. (2022)** results show that the pillar configuration and compressive strength determine the failure mechanism. **Sarfarazi et al. (2023) and Sarfarazi et al. (2021)** show that the non-persistent joint angle and number and the pillar compressive strength governed the failure process. **Fu et al. (2023)** further investigated the effect of joint angle on roof failure by an experimental model where the discontinuity plane was simulated as an edge notch at different angles. It is found that the edge notch angled at 45 degrees has the most critical condition. **Wu et al. 2022** analysed the stability of rib pillars in highwall mining under a static load from overlying strata and a dynamic load from the driving of mining haul trucks for an open pit coal mine in China. Using theoretical calculation and numerical analysis, **Wu et al. (2022)** found that when the opening is 3 m, the width of the rib pillar is a minimum of 1.3 m to ensure its stability. **Jiang, Zhang, et al. 2022** proposed to compute the yield zone width of each side of the web pillar to provide a reasonable pillar width. **Tian et al. (2023)** proposed using a beam structure model to calculate the thickness range of the interlayer and used theoretical calculations to design the web pillar and rib pillar. The results from the proposed equation, theoretical calculation, and numerical modelling showed an agreement. For the case study in the Zhudong coalmine, stability was achieved for a web pillar width of 4.9 m and an interlayer thickness of 1.75 m. Case studies from **Ross et al. 2019; Tian et al. 2023** showed that multi-layer highwall mining is feasible to accomplish sustainable mining.

Coal extraction at the base of the highwall openly causes a weak zone prone to slope failure (**Ross et al., 2019**). The stability of highwall mining depends on the interrelation of the slope and the coal pillars. **Jiang, Lu, et al. 2022** incorporated coal creep behaviour into highwall slope stability analysis. **Ross et al. (2019)** used the limit equilibrium method by Slope W/ to assess the highwall slope stability. **Porathur et al. (2014)** suggested using a simplified 3-D numerical model to assess highwall slope stability for multiple seams mining. **Tabaroei et al. (2022)** elaborated on the advantage of 3D modelling for deep excavation that can produce realistic results of horizontal and vertical displacements.

The practicability of highwall mining in Indonesia is influenced by its weak geological condition (**Sasaoka et al. 2016**). The majority of coal reserves in Indonesia are found in the Tertiary sedimentary basins of Sumatra and Kalimantan (**Friederich and van Leeuwen 2017**). The coal basin has a relatively young geologic age, implying that the rocks are not fully compacted. The intense weathering from a tropical climate and geological structures further weakens the rocks. As a result, the highwall mining system may suffer from stability problems and less coal recovery. Highwall mining is not common in Indonesia, although highwall mining in poor geological conditions is possible, as demonstrated by several cases (**Jiang et al. 2022; Small and Morgenstern 1992; Sasaoka et al. 2016**). Due to maximising marginal reserve, a highwall mining method is proposed for a coal mine in South Kalimantan. Previous studies show that the stability of highwall mining depends on its rock mass condition, coal strength, mine opening and pillar design. It is also shown that the analysis of safe highwall mining utilised a combination of analytical methods and 2D and 3D numerical models. This paper aims to thoroughly assess the stability and dimensions of highwall mining with empirical, analytical and numerical methods at the study location. The outline of this paper begins with an introduction, followed by a brief explanation of the study location and regional geology. The methods employed include an assessment of rock mass condition using Rock Mass Rating (RMR) and Slope Mass Rating (SMR), the collection of geomechanical data from lab testing, and the design of a highwall mining configuration using analytical calculations. 2D and 3D numerical models were used to evaluate the highwall stability. Fur-

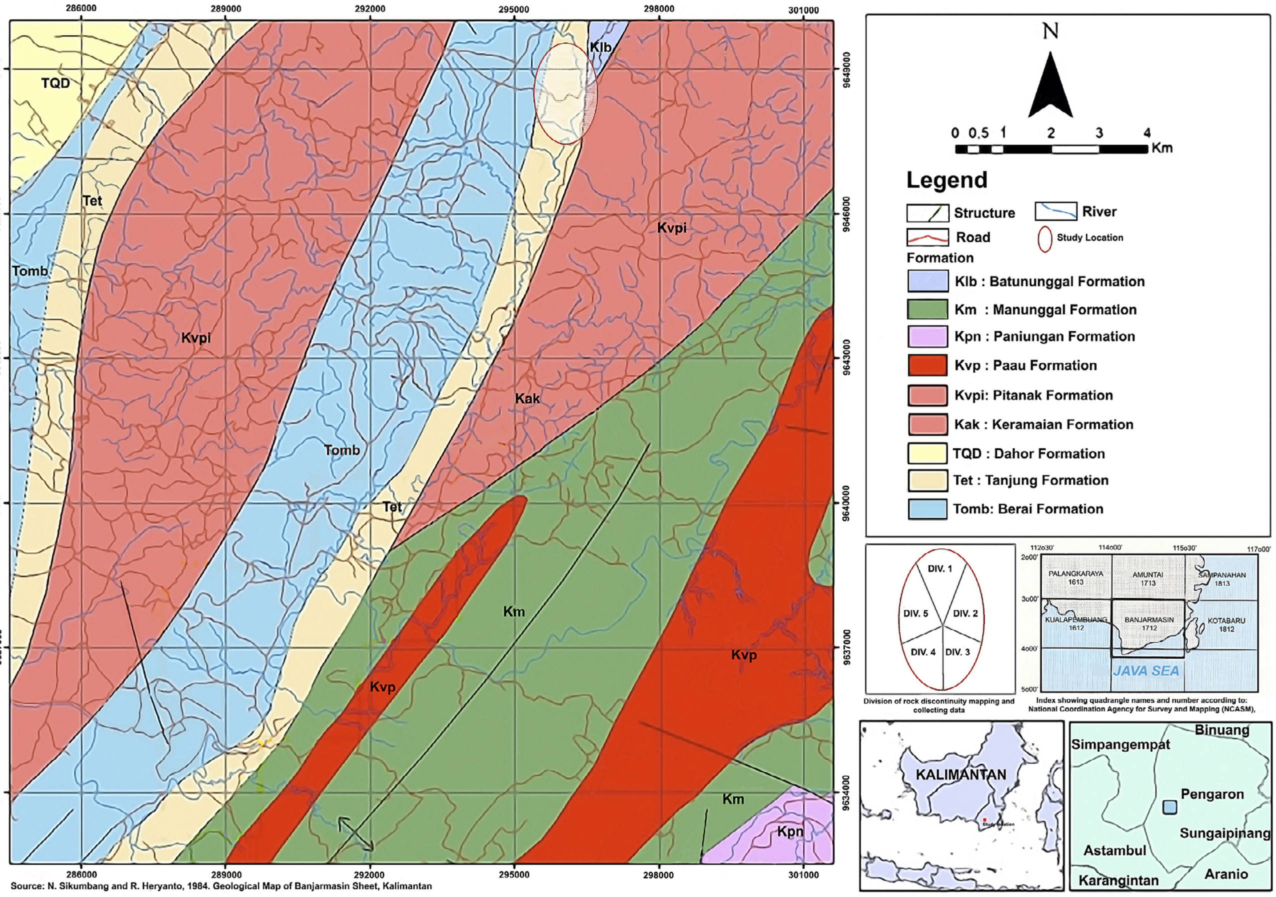

Figure 1: Geological map of the study location

thermore, the coal recovery was also projected for the highwall design. Finally, the results are discussed and the feasibility of highwall mining in a tropical region is shown. This study is limited to the design and stability assessment of the highwall mining. Further implication of the stability condition is discussed but not studied in detail.

2. Study Area and Geological Conditions

This study is conducted in the mining area of PT.X, a coal mine company located 82 km east of Banjarmasin city, South Kalimantan, Indonesia. The coal reserves belong to the Barito Basin, one of Indonesia's main Cenozoic coal-bearing basins (**Friederich and van Leeuwen, 2017**). The Barito Basin was formed by the rifting of the eastern Sunda continental margin, developing a depression filled with transgressive–regressive Tertiary sediment sequences (**Panggabean, 1991**). The basement of the Barito Basin is formed by pre-Tertiary metamorphic rock. The stratigraphy filling the Barito Basin consists of (from old to young) (**Sikumbang and Heryanto, 1994**) the Tanjung Formation (Tet) of Eocene age overlain conformably by the Oligo–Miocene Berai Formation (Tomb). The Middle to Late Miocene Warukin Formation (Tmw) is conformably deposited on top of the Berai Formation. The latter unit is overlain unconformably by the Dahor Formation (TQd). The youngest formation is the alluvial deposit (Qa) of gravel, sand, silt, clay and mud.

The geological structures developed in the area are faults, folds and lineaments, which typically trend NE–SW and NW–SE (**Panggabean, 1991**). Other formations around the research area include the Batununggal Formation (Klb) in the north, Manunggal Formation (Km), Paau (Kvp) and Pitanak Formation (Kvpl) and the Keramaian Formation (Kak). **Figure 1** shows the regional geological conditions of the research area. The Tanjung Formation is the coal-bearing formation in the study area. It has a thickness of up to 750 m and was deposited in a fluvial environment up to shallow seas (**Sikumbang and Heryanto, 1994**). It is composed of alternating sandstone, siltstone and claystone with coal insertions (**Van Bemmelen, 1949; Sikumbang and Heryanto, 1994**).

3. Methods

This study is a new concept that combines empirical, analytical and numerical methods through 2D and 3D modelling to assess the rock mass stability at the mine

 pp. 109-125, DOI: 10.17794/rgn.2023.2.8

site, which will continue from open cut to highwall mining. Rock mass stability is the primary technical issue that needs to be considered to assess whether a site can be developed into a mine location. In this case, slope stability and subsidence are two essential aspects that must be regarded in order to exploit the coal using the highwall method. Lithology, rock structure, slope angle, weathering and groundwater conditions, climate and rock mass characteristics affect rock stability and should be considered when evaluating the possible failure risk. In addition, the pattern and orientation of rock discontinuities at the research site were measured as data for empirical analysis.

Rock mass rating (RMR) and slope mass rating (SMR) are used to classify rock strata at the location as a preliminary evaluation of rock stability. Geotechnical drilling has collected primary data from the area to obtain updated rock samples, which were tested in the geomechanics laboratory. The results of these laboratory tests serve as a reference to determine the physical and mechanical characteristics of each rock type at the research location. This geomechanical data is used as input for modelling software. Furthermore, a simulation of the mine opening design is performed by optimising the acquisition of coal reserves by considering the safety and stability aspects of the rock mass around the mine until post-mining. 2D and 3D models were used to assess surface stability and mine openings.

3.1. Discontinuity observation

Observations and measuring of rock discontinuity patterns have been carried out in five divisions. Some locations are still active with open pit mining, while others are inactive. **Figure 1** includes sites of the divisions. **Figure 2** shows a discontinuity observation and measure at one of the pits. In general, the rocks in the research area consist of sandstone, claystone, mudstone, siltstone and coal. In division 1, the rock layers are generally relatively compact on several slopes. The discontinuity length is < 1 m, spacing is < 60 mm and 200–600 mm, and it is roughly formed. Separation is 0.1 mm with slight weathering, and groundwater is from dry to wet. In division 2, the average layer slope is between 10 and 55 degrees, with a thickness that varies between 0.5 and 50 m. RQD average is 95.2%, the discontinuity length is < 1 m, spacing between joints is 0.25 and 0.25–2 m, and it is roughly formed. Separation is 0.1–1.0 mm, with moderate weathering, and groundwater is dry.

The cracks tend to be closed so that no filling material is found. The level of rock strength is classified from weak rock to hard rock. The outcrops of rocks are as high as 20–30 m, with slopes of about 45–65°. Generally, in division 3, discontinuity length is < 1 m, spacing is about 0.6–2 m, and it is roughly formed. Separation of crack is 1–3 mm, there is no filling material, weathering is slight to moderate, and groundwater is dry and damps locally. Most locations in division 4 have rocks with RQD of 98.5% with a joint spacing of 0.6–2 m and length of about 1–3 m, with roughness being smooth to rough. No filling material was found on the cracks, weathering is slight to moderate, and groundwater is wet to damp. Finally, division 5 has RQD of 98.5%, with most of the discontinuity spacing 0.6–2 m, the length of crack is < 1 m with separation 0.1–1.0 mm, and it is roughly formed. No filling material was found, weathering is slight, and groundwater is wet.

3.2. Rock mass rating

As a starting point for assessing the strength of the rock mass at the research site, Bieniawski introduced the geomechanical classification, namely, the RMR (**Bieniawski, 1973**). Several improvements have been made either by Bieniawski (**Bieniawski, 1978; Bieniawski, 1979; Bieniawski, 1989**) or by other researchers, who proposed revisions to subjective parameters such as roughness and weathering (**Kundu et al., 2020**). RMR has been widely developed for applying technical designs to projects related to earthworks, such as mining, tunnelling, slopes and civil foundations. Rock mass classification is based on several parameters, which include intact rock strength, RQD, discontinuity spacing, discontinuity conditions and groundwater conditions. The evaluation results show the five RMR classifications, namely, very poor (RMR < 20), poor (RMR 40–21), fair (RMR 60–41), good (RMR 80–61) and very good (RMR 100–81). The investigation was carried out at 15 observation stations and spread throughout the pits in the PT.X concession. Every observation conducted in such a way has represented all the rock mass structures that exist in the area. The uniaxial compressive strength test obtains the strength value of intact rock. The RQD value is calculated based on the estimated number of joints or cracks per unit volume (**Palmstorm, 2005**). **Table 1** presents the calculation results obtained from observations with RMR in this study.

Figure 2: Observations and measuring of rock layers and discontinuities

Table 1: RMR value for all station observations at the study area

DIV.	Observation Point	RMR Rating					RMR Value	Class Number	Description
		Rock Strength	RQD	Joint Spacing	Joint Condition	Ground Water Condition			
1	ST-1	2	17	5	27	15	66	II	Good
	ST-2	2	20	5	27	10	64	II	Good
	ST-3	2	20	10	27	7	66	II	Good
2	ST-1	2	20	15	25	15	77	II	Good
	ST-2	2	20	10	24	15	71	II	Good
	ST-3	2	20	10	26	15	73	II	Good
3	ST-1	2	20	15	17	7	61	II	Good
	ST-2	2	20	15	21	10	68	II	Good
4	ST-1	2	20	15	20	15	72	II	Good
	ST-2	2	20	10	23	15	70	II	Good
	ST-3	2	20	15	21	10	68	II	Good
5	ST-1	2	20	15	26	10	73	II	Good
	ST-2	2	20	15	26	10	73	II	Good
	ST-3	2	20	15	26	10	73	II	Good
	ST-4	2	20	15	26	10	73	II	Good

Table 2: SMR results obtained from the study location

No.	DIV.	Observation Point	F1	F2	F3	F4	RMR	SMR	Failure Probability	Stability
1	1	ST 1	0.40	0.40	-6.0	0.0	66	65.04	0.2	Stable
2		ST 2	0.15	1.00	0.0	0.0	64	64.00	0.2	Stable
4			0.15	1.00	0.0	0.0	64	64.00	0.2	Stable
5		ST 3	0.15	0.40	-50.0	0.0	66	63.00	0.2	Stable
6	2	ST 1	1.00	0.70	-25.0	0.0	77	59.50	0.4	Partially unstable
7		ST 2	0.85	0.40	-50.0	0.0	71	54.00	0.4	Partially unstable
8		ST 3	0.15	1.00	-6.0	0.0	73	72.10	0.2	Stable
9			0.15	1.00	0.0	0.0	73	73.00	0.2	Stable
10			0.15	1.00	0.0	0.0	73	73.00	0.2	Stable
11	3	ST 1	0.15	1.00	0.0	0.0	61	61.00	0.2	Stable
12			1.00	1.00	0.0	0.0	61	61.00	0.2	Stable
13			0.40	1.00	0.0	0.0	61	61.00	0.2	Stable
14		ST 2	0.15	0.40	-50.0	0.0	68	65.00	0.2	Stable
15	4	ST 1	0.15	0.40	-6.0	0.0	72	71.64	0.2	Stable
16		ST 2	0.15	1.00	0.0	0.0	70	70.00	0.2	Stable
17			0.40	1.00	0.0	0.0	70	70.00	0.2	Stable
18			0.15	1.00	0.0	0.0	70	70.00	0.2	Stable
19		ST 3	0.15	1.00	0.0	0.0	68	68.00	0.2	Stable
20			0.15	1.00	0.0	0.0	68	68.00	0.2	Stable
21	5	ST 1	0.70	0.40	-60.0	0.0	73	56.20	0.4	Partially unstable
22		ST 2	0.15	1.00	0.0	0.0	73	73.00	0.2	Stable
23			0.40	1.00	0.0	0.0	73	73.00	0.2	Stable
24		ST 3	0.15	0.15	-60.0	0.0	73	71.65	0.2	Stable
25		ST 4	0.15	1.00	0.0	0.0	73	73.00	0.2	Stable
26			0.15	1.00	0.0	0.0	73	73.00	0.2	Stable

3.3. Slope mass rating

Highwall mining is transitional mining from open pit to underground mining. Therefore, in addition to the stability of underground openings, it also involves slope stability. Hence, safety considerations on slopes around highwall mines need to be considered. RMR assessment still poses some difficulties when applied to the valuation of slope stability because the parameters that consider the influence of discontinuity orientation are generally more to specific conditions such as underground mines, tunnels and dam foundations projects while viewing slope stability still requires several other parameters (**Aksoy, 2008**). **Romana (1985)** introduced the slope mass rating (SMR), which is still based on the parameters of Bieniawski. This concept is popular and widely used to assess the stability of slopes. The Romana concept has added four factorial adjustments, namely, F1, F2, F3 and F4. F1, F2 and F3 are adjustment factors that depend on the orientation of discontinuity and slope, and F4 is the factor for the adjustment that depends on the exploitation method.

$$SMR = RMR + (F1xF2XF3) + F4 \tag{1}$$

The SMR value ranges from 0 to 100 with five different stability categories that thoroughly consider potential failure and probability of failure. **Table 2** presents the result of calculating the SMR value in the study area.

Based on the RMR analysis as shown in **Table 1**, the RMR value of the study location is included in class II (Good). Meanwhile, from the results of the SMR analysis shown in **Table 2**, the rock strata for each division are stable, except for station 1 (ST 1) in division 5. From these two analyses, prior to excavation with the highwall mining, the rock strata is relatively stable.

3.4. Analytical calculation and numerical modelling

Numerical modelling was performed using two software, i.e., RS2-Rocscience for 2D and Ansys for 3D modelling. The Mohr–Coulomb failure criteria were used in the analysis since the rock mass consists of many layers. This criterion is known for its ease of mathematical formulation. Mohr's envelope is considered to be a straight line, and its equation is expressed as the Mohr–Coulomb criterion by the following equation:

$$\tau = c + \mu\sigma \tag{2}$$

where τ is shear strength, σ is normal stress, c is cohesion and μ is the internal friction coefficient of the rock or tan ϕ. The Mohr–Coulomb (MC) failure criterion can be expressed using major and minor principal stress terminology, such as explained in the following equation:

$$\sigma_1 = \sigma_3 \frac{1+sin\varphi}{1-sin\varphi} + \frac{2c\ cos\varphi}{1-sin\varphi} \tag{3}$$

σ_1 and σ_3 show the major and minor principal stress values, respectively, c is cohesion and ϕ is the internal friction angle. The linear regression analysis has been used traditionally to determine the power parameters c and φ and generally has been found to produce perfect results. The value of the unconfined compressive strength (UCS) (σ_c) is predicted through:

$$\sigma_c = \frac{2c\ cos\varphi}{1-sin\varphi} \tag{4}$$

In terms of the principal stress, the Mohr–Coulomb failure criterion can be expressed as a safety factor value by the following equation:

$$SF = \frac{1}{2}(\sigma_1 - \sigma_3) + \frac{1}{2}(\sigma_1 + \sigma_3)sin\vartheta - c\ cos\vartheta = 0 \tag{5}$$

The equation can be expressed as stress invariants the Mohr- Coulomb yield surface is:

$$SF = \frac{I_1}{3}\sin(\vartheta) + \sqrt{I_2}\left[\cos(\theta) - \frac{1}{\sqrt{3}}\sin(\theta)\sin(\vartheta)\right] - c\ cos(\vartheta) = 0 \tag{6}$$

I_1 and I_2 are the expressed stress invariants. On the plastic zone, the function has the same form as the yield surface that is expressed in the following equation:

$$Q = \frac{I_1}{3}\sin(\psi) + \sqrt{I_2}\left[\cos(\theta) - \frac{1}{\sqrt{3}}\sin(\theta)\sin(\vartheta)\right] - c\ cos(\psi) = constant \tag{7}$$

where ψ is the dilation angle which should be less or similar to the residual friction angle; RS2 accepts peak and residual values for the cohesion and friction angle. In RS2, the Mohr–Coulomb model can be assigned as an elastic–brittle–plastic material model. In the case where the residual values are the same as peak values, the behaviour is elastic–perfect–plastic. In 3D modelling using Ansys software, the hexagonal failure surface of Mohr–Coulomb (MC) combines with the cone Drucker–Prager (DP) failure. The pressure-dependent model specifies whether a rock mass has failed or is in the plastic zone (**Drucker and Prager, 1952**). The Drucker–Prager yield function is expressed as:

$$f(\sigma) = k = \alpha I_1 + \sqrt{I_2} \tag{8}$$

where k and α express cohesion *c* and internal friction angle ϕ properties of the intact rock, respectively, and are defined as

$$k = \frac{6\sqrt{3}c\ cos\varnothing}{\sqrt{2\sqrt{3}\pi(9-\sin^2\varnothing)}},\ \text{and}\ \alpha = \frac{2\sqrt{3}sin\varnothing}{\sqrt{2\sqrt{3}\pi(9-\sin^2\varnothing)}} \tag{9}$$

the yield surface on the deviatoric plane is the equivalent area circle of the hexagon. It is called Mohr-Coulomb equivalent area circle criterion and it call a smooth surface yield MC criterion. In the DP yield model, to assess

Table 3: Physical properties

No	Lithology	Layer thickness	Natural Density	Saturated Density	Dry Density	Natural Water Content	Saturated Water Content	Degree of Saturation	Porosity	Void Ratio	Slake Durability
		(m)	(MN/m^3)	(MN/m^3)	(MN/m^3)	(%)	(%)	(%)	(%)	(%)	(%)
1	Claystone	0.20	0.0238	0.0241	0.0227	5.07	6.56	77.41	15.17	0.18	13.58
2	Siltstone	8.39	0.0242	0.0246	0.0232	3.95	5.49	71.85	13.04	0.15	65.74
3	Sandstone	11.24	0.0236	0.0239	0.0226	4.70	5.79	81.64	13.31	0.15	96.59
4	Claystone	12.84	0.0233	0.0235	0.0220	6.13	7.08	86.58	15.86	0.19	98.27
5	Sandstone	12.98	0.0218	0.0219	0.0198	9.99	10.80	92.59	21.76	0.28	95.63
6	Siltstone	12.05	0.0244	0.0247	0.0237	2.91	3.98	73.26	9.69	0.11	90.02
7	Sandstone	11.46	0.0231	0.0234	0.0219	5.97	6.97	85.89	15.55	0.18	78.23
8	Siltstone	7.05	0.0250	0.0252	0.0242	3.13	4.22	74.11	10.42	0.12	89.32
9	Sandstone	7.03	0.0218	0.0221	0.0196	10.89	11.98	90.93	24.02	0.32	94.39
10	Cl. Sandstone	13.90	0.0242	0.0245	0.0234	3.37	4.28	79.26	7.01	0.08	98.89
11	Coal - C	3.43	0.0145	0.0147	0.0140	3.37	4.92	74.62	7.01	0.08	98.89
12	Coaly-clay	1.14	0.0230	0.0234	0.0223	3.76	5.16	72.97	11.69	0.13	83.87
13	Claystone	31.30	0.0232	0.0245	0.0227	3.37	4.28	79.26	7.01	0.08	98.89
14	Coal - D	2.80	0.0125	0.0126	0.0121	3.43	4.21	81.17	5.17	0.05	96.92
15	Claystone	94.11	0.0237	0.0240	0.0228	4.44	5.46	81.45	12.65	0.14	27.36

Table 4: Mechanical properties

No.	Lithology	Layer thickness	UCS				Triaxial Comp. Strength		Direct Shear (Residual)	
		(m)	Tensile MPa	σ_c (MPa)	E (MPa)	μ	ϕ_p(°)	Cp (MPa)	ϕ_r	C_r (MPa)
1	Claystone	0.20	1.19	3.47	461.29	0.23	23.10	1.06	4.29	0.12
2	Siltstone	8.39	1.46	3.61	988.74	0.43	23.60	1.40	8.73	0.06
3	Sandstone	11.24	1.69	2.54	900.64	0.36	49.61	1.26	14.83	0.07
4	Claystone	12.84	3.45	53.16	8959.24	0.46	52.82	8.25	10.04	0.11
5	Sandstone	12.98	2.66	11.54	1678.37	0.38	42.25	3.91	9.49	0.10
6	Siltstone	12.05	2.28	5.50	2576.52	0.27	46.90	0.90	27.61	0.02
7	Sandstone	11.46	1.73	12.68	1736.97	0.45	50.89	4.36	15.59	0.12
8	Siltstone	7.05	2.47	5.00	1686.81	0.36	46.22	2.28	13.99	0.08
9	Sandstone	7.03	1.44	22.68	2252.49	0.33	35.27	4.00	11.25	0.12
10	Cl. Sandstone	13.90	3.27	19.40	2905.11	0.36	39.79	8.36	24.39	0.03
11	Coal - C	3.43	1.75	11.41	1316.96	0.33	31.03	1.73	21.77	0.06
12	Coaly-clay	1.14	1.90	3.36	794.04	0.38	46.45	0.34	10.47	0.05
13	Claystone	31.30	1.15	2.05	322.00	0.33	38.69	1.27	8.90	0.08
14	Coal - D	2.80	1.59	6.32	958.87	0.38	31.03	2.50	19.41	0.07
15	Claystone	94.11	1.41	3.12	905.48	0.34	28.91	1.35	8.40	0.08

the safety factor it can be expressed by a strength reduction coefficient such as:

$$F = \frac{k}{SF} = \frac{\sigma}{SF} I_1 + \sqrt{I_2} \qquad (10)$$

The SF variable is a safety factor when the rock mass attains the limit state to undergo failure. The yield surface of DP is the refinement of the MC yield surface that is expressed as:

$$I_1 = \sigma_1 + \sigma_2 + \sigma_3 \text{ and}$$

$$I_2 = \frac{1}{6}\left[\left(\sigma_1 - \sigma_2\right)^2 + \left(\sigma_1 - \sigma_3\right)^2 + \left(\sigma_2 - \sigma_3\right)^2 \right] \qquad (11)$$

where k and α express the intact rock's cohesion and internal friction properties, respectively. If the variable α is set to 0, the DP criterion reduces to Von Mises criterion. Of these several variations, the efficiency will bring a lot of convenience to numerical calculations.

3.4.1. Data input

The physical and mechanical properties for every layer in sections 1–5 were used as the input data for this two software. All rock layer materials that make up the model are based on the characterisation of the rock mass as a result of laboratory tests. The geotechnical data is taken from the average parameter values from the site around sections. Generally, the rocks in the research area are claystone, sandstone, mudstone and coal. The geomechanics tests consisted of physical and mechanical properties using the Indonesian National Standard (SNI). These properties include density, porosity and void ratio (**SNI 03-2437-1991**), slake durability (**SNI 3406:2011**), uniaxial compressive strength (UCS) (**SNI 2825:2008**), direct shear (**SNI 2824:2011**) and triaxial (**SNI 2815:2011**) tests. **Tables 3** and **4** summarise the physical and mechanical properties of the rock layers. The thickness of the rock layers in the modelling is adjusted to the actual thickness based on the correlation between drill holes in the study area, as seen in **Figure 3**.

3.4.2. Model design

After all surface coal has been mined, highwall mining will begin on the final slope with slope conditions like cross-section 5 (see **Figure 3**). Mined coal seams are 3.43 m and 2.8 m thick. The results of the RMR and SMR studies indicate that the rock mass quality is included in category II or the "Good" class. A 2D and 3D slope model was developed by combining the AutoCAD drawings of the topography on cross-section 5 in **Figure 3** using RS2 and ANSYS to represent 15 material layers forming the strata, including coal seams C and D. The physical and mechanical properties are reflective of the rock layers. In the model, the gravitational stress is regarded as the original rock stress fields. Boundary conditions are essential for defining a boundary value problem to avoid boundary effects in numerical analysis (Zwillinger, 2014). The upper boundary of the model is free, and the lower boundary is fully constrained. In 2D models, the left and right boundaries, the X-axis is constrained, and the Y-axis is free. The 2D model has dimensions Y: 230 m (height) and X: 343 m (width). The distance between model boundaries is 122 m from the object excavation or 35 times the width of the object excavation. In 3D models, on the sides of the model, the X-axis is constrained, the Y-axis is free (in Ansys called frictionless support), the bottom is fully constrained (in Ansys called fixed support), and the surface that follows topographical conditions is free. The 3D model has dimensions Y: 230 m (maximum height), X: 343 m (length) and Z: 173 m (width). The distance between the model's boundary to the object excavation is about 50m or 14 times the width of the excavation object.

Analytically, a simple calculation has been carried out using the following equation (**Zipf, 2005; Zipf and Mark, 2005**):

$$FoS_W = \frac{\sigma_{coal}\left[0.64 + 0.54 \, {}^{W_W}\!/_{h_{op}}\right]}{\left[\dfrac{0.025H\left(W_W + W_{op}\right)}{W_W}\right]} \tag{12}$$

where FoS_W is the safety factor of the web pillar, σ_{coal} is the strength of coal (MPa), W_W is the width of the web pillar (m), W_{op} is the width of the mine opening, h_{op} is the coal seam thickness and 0.025H is the average vertical stress of overburden height (MPa).

$$W_{PN} = n\left(W_W + W_{op}\right) + W_{op} \tag{13}$$

$$FoS_{BP} = \frac{\sigma_{coal}\left[0.64 + 0.54 \, {}^{W_{BP}}\!/_{h_{op}}\right]}{\left[\dfrac{0.025H\left(W_{PN} + W_{BP}\right)}{W_{BP}}\right]} \tag{14}$$

where W_{PN} is the width of the panel, n is the number of web pillars in the panel, FoS_{BP} is the safety factor of the barrier pillar, and W_{BP} is the width of the barrier pillar**.** **Equations 12**, **13** and **14** can calculate the widths of the web pillar, barrier pillar and mine opening (Wop). This dimension certainly should be adjusted to the provisions for the safety factor > 1. The height (H) of the model is adjusted to the thickness of the strata above the mined coal seam. For the mining geometry and safety factor calculation on coal Seam-C, the layers are 97.55 m (calculated from the highest elevation) and 88.72 m thick, while on coal Seam-D, the layers are 133.63 m and 124.58 m thick. Ten models are presented in this study by simulating the thickness of rock strata (H), the thickness of coal taken (hop), the width of openings (Wop), the width of web pillars (Ww), the width of barrier pillar (W_{BP}) and the number of web pillars in the panel (n). This simulation aims to obtain the most optimal value, calculated using analytical and numerical models. **Table 5** presents the parameters of the highwall mining simulation.

The results of these analytic calculations are simulated together by numerical modelling. The shape of the final slope, rock mass strata and highwall mine opening was illustrated based on the cross-section of the site conditions. **Figures 4** and **5** show the front and side views of the model to be simulated using numerical modelling.

3.4.3. Data analysis

The geometry of the mine opening, material properties and field stress properties are the data needed for

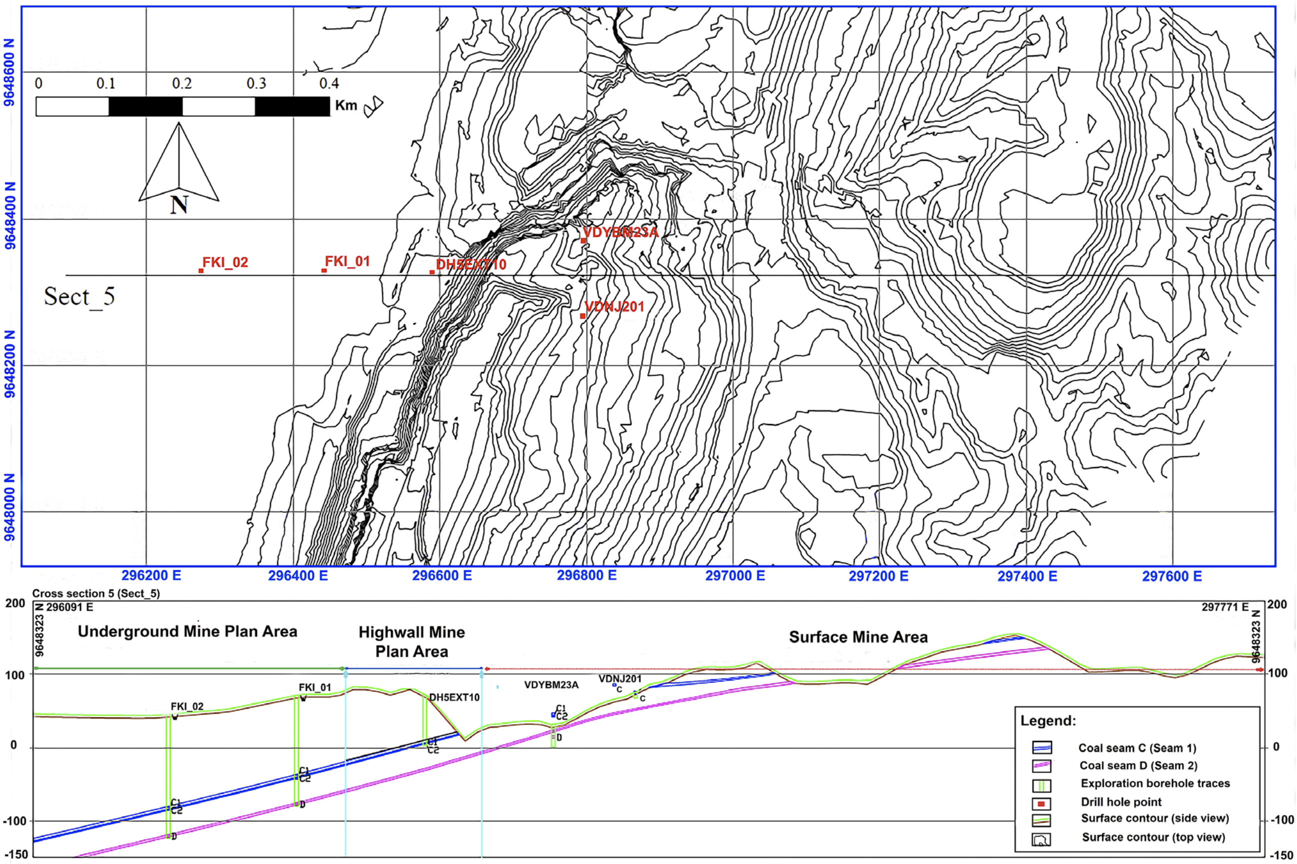

Figure 3: Coal and surface condition of slope on cross-section 5

Table 5: Analytical simulation of highwall mining parameters

Sim.	h_{op} (m)	H (m)	W_{op} (m)	W_W (m)	W_{BP} (m)	n	W_{PN} (m)	h_{op} (m)	H (m)	W_{op} (m)	W_W (m)	W_{BP} (m)	n	W_{PN} (m)
	Coal Seam-C							**Coal Seam-D**						
1	3.43	97.55	3.50	2.00	3.00	5	31.00	2.80	133.63	3.00	3.50	4.00	4	29.00
2	3.20	97.55	3.50	2.00	3.00	5	31.00	2.50	133.63	3.00	3.50	4.00	4	29.00
3	3.20	97.55	3.50	2.50	3.00	5	33.50	2.50	133.63	2.50	3.50	4.00	4	26.50
4	3.20	97.55	3.00	3.00	4.00	5	33.00	2.50	133.63	3.00	4.00	4.50	4	31.00
5	3.20	97.55	3.50	2.00	3.00	4	25.50	2.50	133.63	3.00	3.50	4.00	3	22.50
6	3.20	97.55	3.00	2.50	3.00	4	25.00	2.50	133.63	2.50	3.50	4.00	3	20.50
7	3.20	97.55	3.00	3.50	4.00	4	29.00	2.50	133.63	3.00	3.50	4.00	4	29.00
8	3.20	88.72	3.00	2.00	3.00	4	23.00	2.50	124.58	3.00	4.00	4.50	3	24.00
9	3.20	88.72	3.50	2.00	3.00	5	31.00	2.50	124.58	3.00	3.50	4.00	4	29.00
10	3.20	88.72	3.00	3.00	4.00	5	33.00	2.50	124.58	3.00	4.00	4.50	4	31.00

numerical modelling. In 2D modelling, the highwall mine opening segment is simulated at the highest load indicated by the thickest rock strata above coal Seam-C and coal Seam-D. Meanwhile, in the 3D model, the highwall mine opening is 150-m long, and the load is adjusted according to topographic conditions. There is at least one panel flanked by two barrier pillars and several web pillars outside the panel, as shown in **Figure 6.**

The boundary conditions on the sides of the model are determined at least once by the width of the mining area, which is calculated from the outer boundary of both sides of the mining area. The upper limit is the thickness of the overburden of highwall mining, which is 97.55 m when calculated from coal Seam-C, 133.63 m from coal Seam-D and 230 m from the lower limit of the model. An upper part of the boundary conditions was applied as

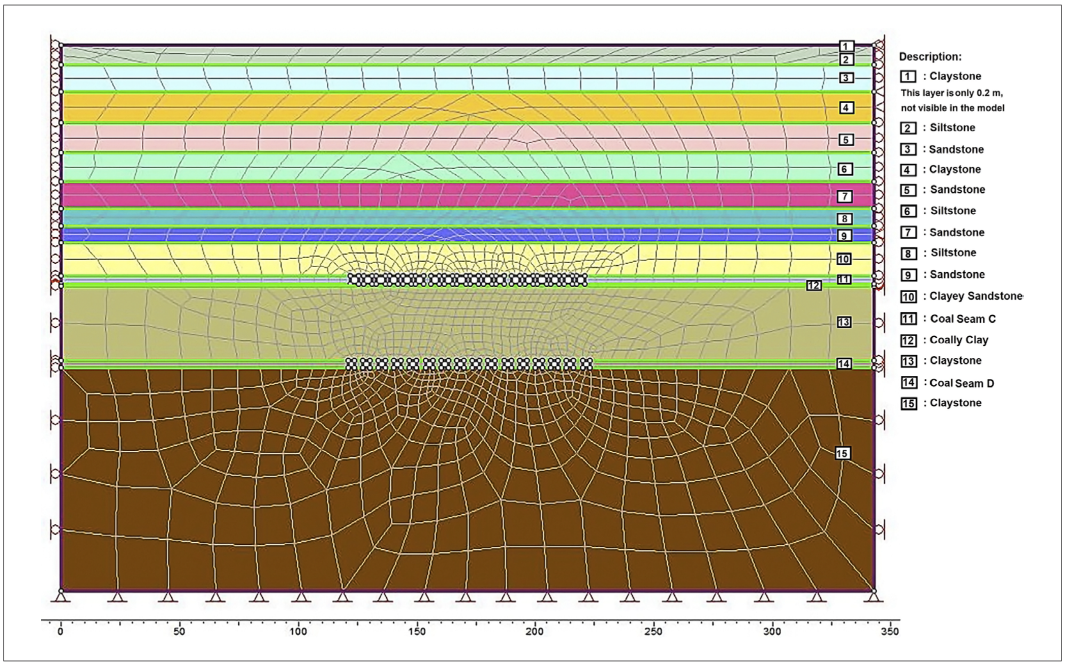

Figure 4: 2D Model (RS2)

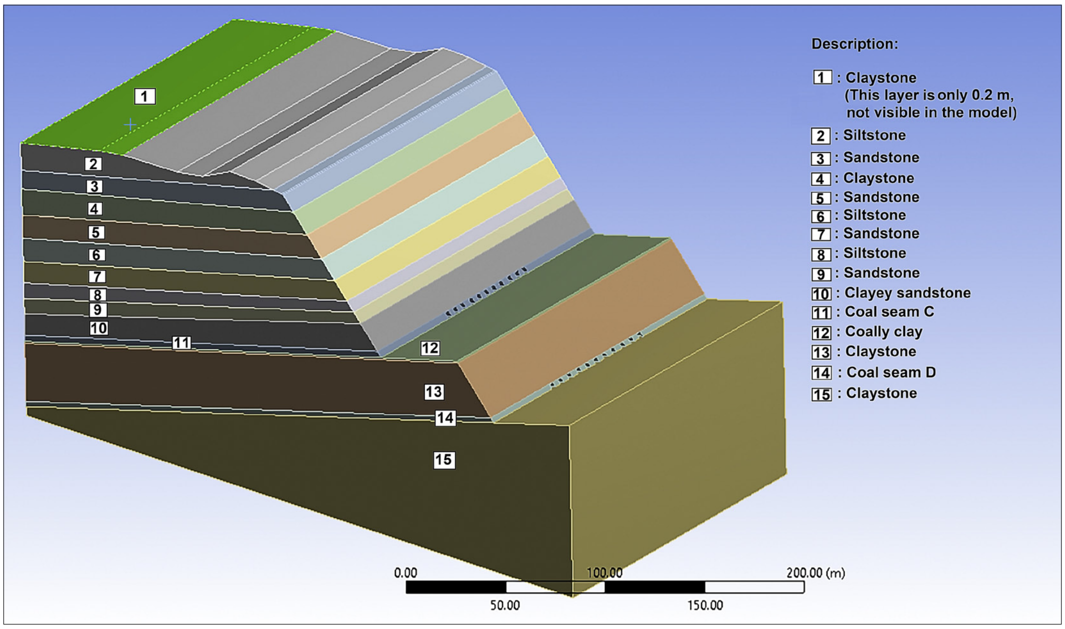

Figure 5: 3D Model (Ansys)

the free restraint, which meant that displacement was permitted in all directions on the surface. On both modelling sides, the control is in the horizontal direction, and the approved deformable plane is only on the vertical axis. The bottom part of the boundary conditions does not allow displacement in all orders. Appropriate restraint application of boundary conditions in numerical modelling can affect the displacement occurrence.

The standard loads applied are field stress and seismic load in 2D models RS2 or standard earth gravity and acceleration in 3D models Ansys. Field stress properties are needed to determine the occurrence of in situ stress conditions before mining. The stress is defined in vertical and horizontal directions. The field stress type in RS2 consists of constant and gravity types, and the study models have chosen the gravity type. The value of the ratio between the horizontal stress to the vertical stress (k) is set as the input parameter.

Furthermore, the geometric model must be divided into more minor elements so that calculations can be carried out using the finite element method. The composition of these elements is referred to as mesh elements. The RS2 software (Rocscience, Inc.) has four types of mesh elements: three-noded triangles, six-noded trian-

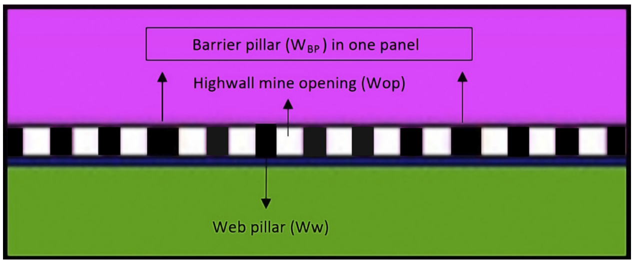

Figure 6: Geometry model of highwall mine opening

gles, four-noded quadrilaterals and eight-noded quadrilaterals with graded, uniform and radial mesh types. The finer the mesh used, the more accurate the results obtained, but the calculation time and the required file size will also increase. In this study, the appropriate type of element and mesh is to use six-noded triangles and graded. In contrast, 3D Ansys modelling automatically controls modelling and producing about 107,600 nodes and 31,100 elements.

After all the required parameters are entered into the programme, the next step is calculating the numerical analysis. The calculation results obtained are interpretations of graphical data in the form of values such as total displacement, strength factor, effective stress, total stress, strain and plastic strain on 2D RS2 models. Meanwhile, the 3D Ansys models obtained values such as total deformation, safety factor, direct deformation, equivalent strain and stress (Von Mises), and maximum and minimum strain or stress and strain energy, among others. Furthermore, only the total displacement and strength factor on the 2D RS2 models and the total deformation and safety factor on the 3D Ansys models are used to evaluate the stability of the mining area. **Figure 7a** and **7b** show an example of interpreting the total displacement and strength factor values in a 2D model using RS2 software. **Figure 8a** and **8b** show the total deformation and safety factor values using the Ansys software in the area around the highwall mine opening. Both 2D dan 3D models, as shown in **Figure 7** and **Figure 8**, use plane strain analysis. This analysis can solve a wide range of elasticity equations in 2D and 3D and is a precise solution. In comparison, plane stress assumes that normal stresses and shears perpendicular to the model are equal to zero. Therefore, it is only appropriate for a thin model but not suitable for 3D models. Stress analy-

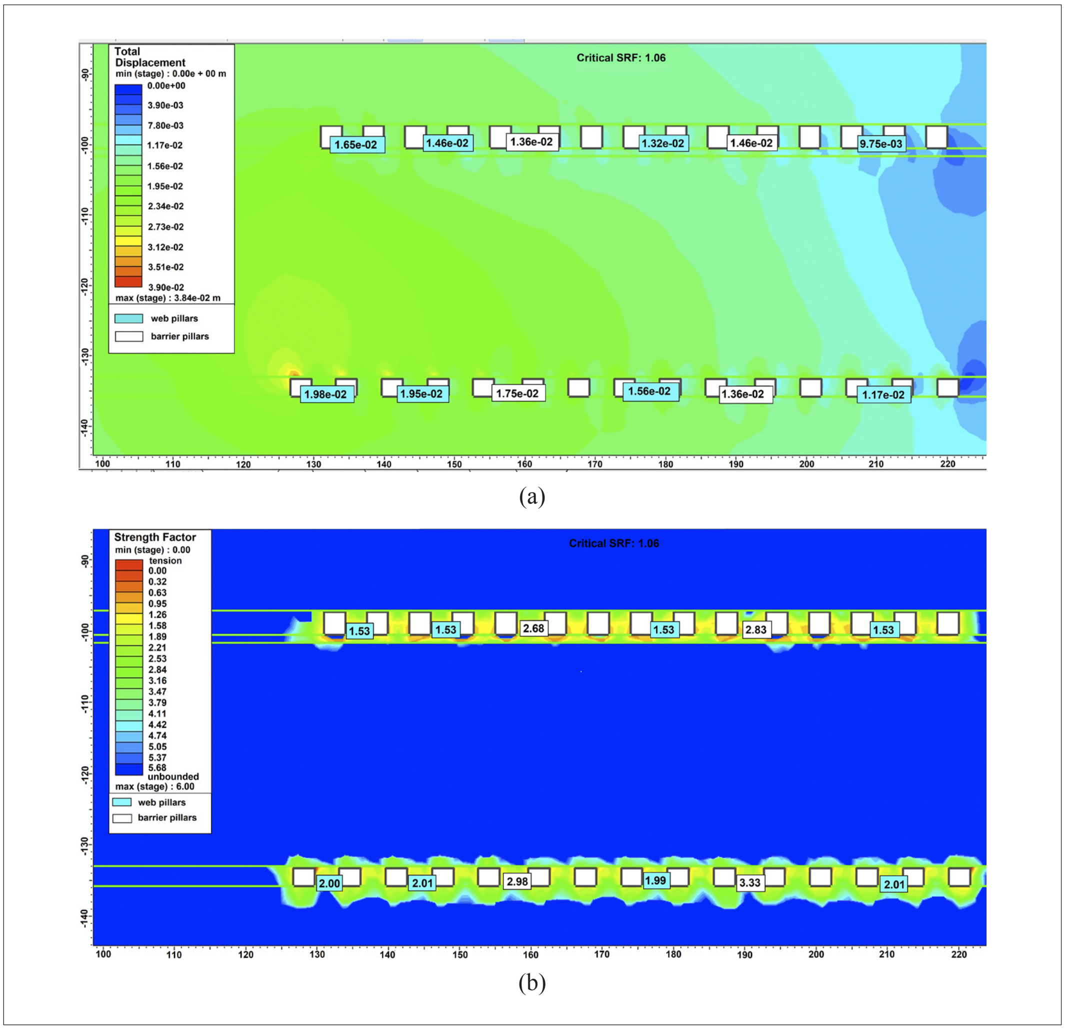

Figure 7: (a) One of the displacement models and **(b)** strength factor in 2D using RS2

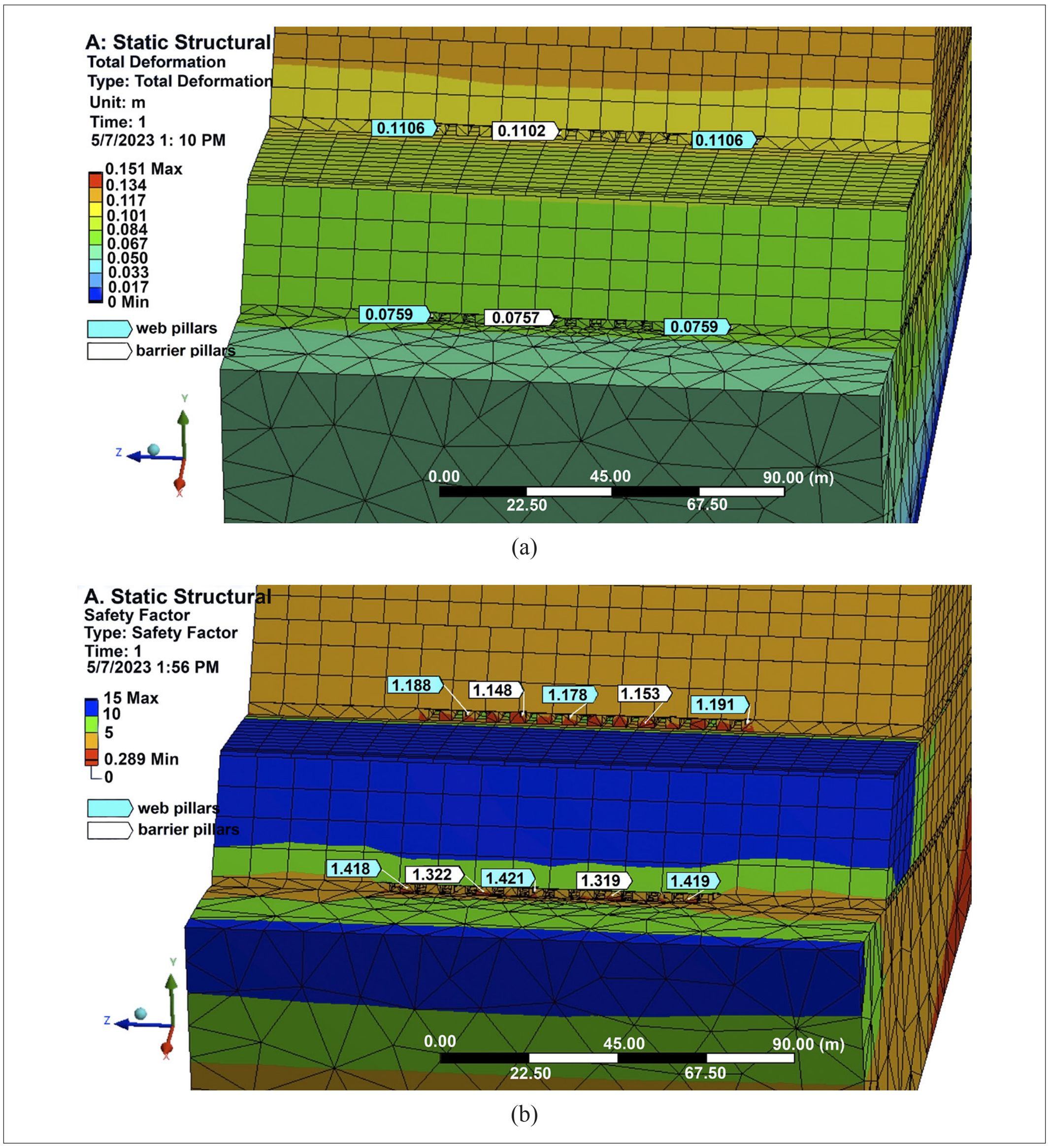

Figure 8: **(a)** One of the deformation models and **(b)** safety factor in 3D using Ansys

sis used a maximum number of iterations of 1000 with a tolerance of 0.001. **Figure 7a** shows the maximum displacement value in the model is 0.039 m, with an average displacement value on web pillar and barrier pillar is 0.0135 m and 0.0141 respectively on seam C and 0.0167 m and 0.0156 respectively on seam D. Meanwhile, **Figure 7b** shows the value of the strength factor with an average strength factor on the web pillar and barrier pillar is 1.53 and 2.76 respectively on seam C and 2.00 and 3.16 respectively on seam C at the conditions of strength reduction factor (SRF) 1.06. **Figure 8a** shows the maximum deformation value of 0.151 m and the average deformation of the web pillar and barrier pillar is 0.1106 m and 0.1102 m, respectively, on-seam C, and 0.0759 m and 0.0757, respectively, on-seam D. **Figure 8b** shows an average safety factor on the web pillar and barrier pillar is 1.19 and 1.15 on coal seam C and 1.42 and 1.32 respectively on seam D.

4. Result and Discussion

The stage of evaluating the feasibility of the location for highwall mining has been carried out, which started with assessing the strength of the rock mass using the RMR and SMR approaches. The evaluation results show that most rock strata are stable prior to mining, and only a few places show partially unstable conditions (see **Table 2**). Furthermore, an analytic approach was used to evaluate the stability of the top surface, highwall faces and entry roofs, such as the height and width of mine opening, the width of web pillars and the width of barrier pillars. After that, the models were simulated by 2D and 3D numerical methods RS2 and Ansys software.

This modeling and simulation of the stability of mine openings and the surface of the mining area are carried out to determine the optimum value of carrying capacity and safety factors for mining. Several models have been

Table 6: Safety factor and total displacement/deformation in the web pillar and barrier pillar at coal seam-C

Sim.	Analytic		2D – RS2 (Average)				3D – Ansys (Average)			
	Safety Factor		Displacement (m)		Strength factor		Deformation (m)		Safety factor	
	FoS_W	FoS_{BP}	web	BP	Sf_{web}	Sf_{BP}	web	BP	Sf_{web}	Sf_{BP}
1	1.62	2.28	0.2534	0.2330	1.03	0.95	0.1099	0.1100	0.68	0.74
2	1.66	2.42	0.1232	0.1603	1.58	1.34	0.1102	0.1096	0.75	0.91
3	2.07	2.42	0.1260	0.1103	1.42	1.19	0.1102	0.1099	0.90	1.14
4	2.68	3.14	0.1590	0.1450	1.71	1.46	0.1104	0.1100	1.17	1.19
5	1.66	2.43	0.0813	0.0975	1.79	1.42	0.1106	0.1115	0.92	1.04
6	2.26	2.44	0.0975	0.1560	1.37	1.89	0.1106	0.1101	1.01	1.12
7	3.10	3.14	0.0135	0.0141	1.53	2.76	0.1106	0.1102	1.19	1.15
8	2.01	2.68	0.0141	0.0136	1.58	2.92	0.1095	0.1096	0.92	1.12
9	1.83	2.66	0.2013	0.2538	0.95	1.03	0.1098	0.1095	0.80	1.07
10	2.95	3.45	0.1595	0.1378	1.05	0.95	0.1097	0.1097	1.07	1.18

Table 7: Safety factor and total displacement/deformation in the web pillar and barrier pillar at coal seam-D

Sim.	Analytic		2D – RS2 (Average)				3D – Ansys (Average)			
	Safety Factor		Displacement (m)		Strength factor		Deformation (m)		Safety factor	
	FoS_W	FoS_{BP}	web	BP	Sf_{web}	Sf_{BP}	web	BP	Sf_{web}	Sf_{BP}
1	1.34	1.43	0.1530	0.0855	2.39	2.69	0.0755	0.0759	1.52	1.36
2	1.42	1.58	0.0959	0.0823	1.97	2.21	0.0757	0.0755	1.58	1.37
3	1.54	1.58	0.0910	0.0368	2.08	2.21	0.0759	0.0755	1.81	1.51
4	1.63	1.76	0.0894	0.0759	2.22	2.37	0.0758	0.0755	1.58	1.47
5	1.42	1.57	0.0802	0.0731	2.10	2.53	0.0758	0.0758	1.64	1.44
6	1.54	1.57	0.0845	0.0975	1.96	2.69	0.0756	0.0758	1.82	1.51
7	3.10	3.14	0.0167	0.0156	2.00	3.16	0.0759	0.0757	1.42	1.32
8	1.74	1.87	0.0166	0.0171	2.64	3.24	0.0753	0.0752	1.41	1.41
9	1.53	1.70	0.0933	0.0788	2.16	2.21	0.0755	0.0751	1.49	1.52
10	1.74	1.89	0.0773	0.0725	2.42	2.45	0.0757	0.0754	1.63	1.69

simulated to find the optimum highwall mining geometry. In the end, the potential amount of coal extracted is also evaluated compared to the remaining coal after mining. **Tables 6** and **7** show results from ten model variations by analytical, 2D, and 3D numerical modeling simulations for seam-C and seam-D. The results represent changes in the total displacement/deformation and safety factor values after excavation. The interpretation results evaluate a set of high wall mine openings consisting of a hole mine, web pillars, and barrier pillars.

Three parameters are simulated, such as the maximum width of the mine opening (W_{op}) and the minimum of the web pillars and barrier pillars (W_w and W_{BP}), with a safety factor value of > 1, which are the primary assessment criteria. Ten variations of parameters have been simulated on coal seam-C and coal seam-D to determine the value of the safety factor on the web pillars and barrier pillars (FoS_w and FoS_{BP}) using analytical methods and 2D and 3D numerical models. Numerical modelling also evaluates the displacement or deformation of the entire model.

Based on the simulation results for ten variations of highwall mining dimensions in coal Seam-C, presented in **Tables 5** and **6**, the most optimum highwall geometry is obtained in the seventh simulation. The geometry dimension of the coal thickness is 3.20 m, the width of the mine opening is 3.00 m, and the widths of the web pillar and the barrier pillar are 3.50 m and 4.00 m, respectively, with four web pillars in one panel. In coal Seam-D, the optimum geometry is still chosen from the seventh simulation presented in **Table 7**, with a coal thickness of 2.50 m, mine opening width of 3.00 m, and web pillar and barrier pillar widths of 3.5 m and 4.00 m, respectively, with four web pillars in one panel.

Figures 7 and **8** represent deformation and safety factors for 2D and 3D analysis on the seventh simulation in **Table 6** and **7**. Even though the calculation results show the safety factor > 1 and small displacement and deformation in 2D and 3D models, some pillars on seam C are not very strong (see **Figure 7b** and **Figure 8b**). Therefore, when mining, it is necessary to prepare suitable excavation stages. Sequential excavation must be implemented by digging in a coal seam with a higher pillar strength first. Prioritizing mining on coal seam D is suggested because the stability of the pillars on this seam is better than seam C. Furthermore, for coal excavation on seam C, besides implementing sequential excavation, it is also necessary to take action by inserting filling material into the holes that have been mined.

The percentage of coal that can be mined (recovery of coal excavation) will be known by comparing the dimensions of the mine opening (Wop) with the web pillars and barrier pillars. Based on the highwall dimension

 pp. 109-125, DOI: 10.17794/rgn.2023.2.8

parameters for the selected coal Seam-C, theoretically, the percentage of the recovery obtained is:

$$\frac{5(hole)x3m(W_{op})}{5(hole)x3m(W_{op})+\left[4(panel)x3.5m(W_{w})+2(barrier\ panel)x4m(W_{BP})\right]}x100\% = 40.54\% \tag{15}$$

As for coal seam-D, theoretically, the percentage of coal excavation recovery is:

$$\frac{5(hole)x3m(W_{op})}{5(hole)x3m(W_{op})+\left[4(panel)x3.5m(W_{w})+2(barrier\ panel)x4m(W_{BP})\right]}x100\% = 40.5\% \tag{16}$$

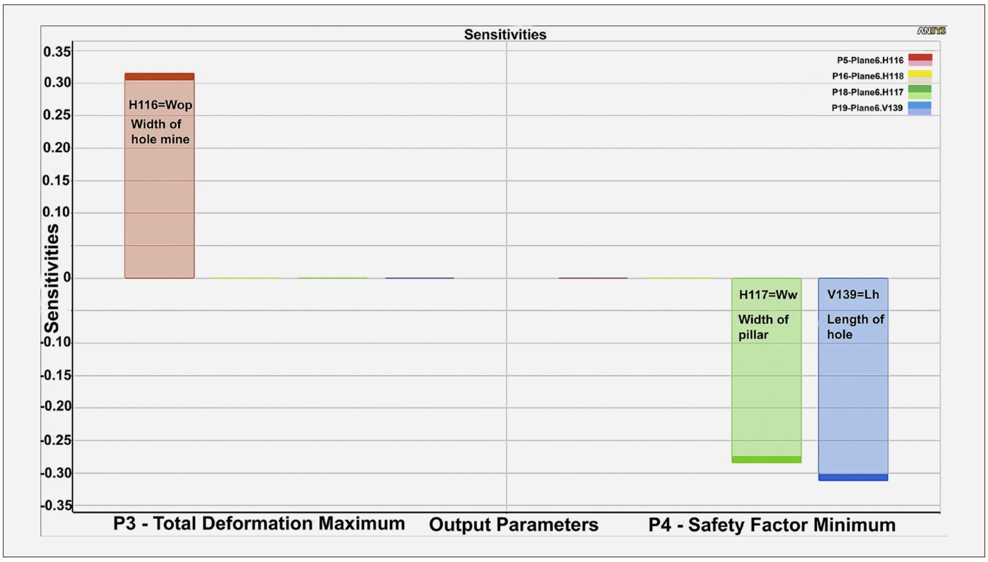

Figure 9: Sensitivity analysis of W_{op}, W_w, W_{BP} and Lh versus the total deformation and safety factor

Highwall mining cannot be separated from the influence of the condition of the geological structure, rock strata, rock mass properties and roof and floor rock of coal seam targets, which are some of the parameters that affect the stability of the highwall. In addition, the key parameters that directly affect the stability are the dimensions of the highwall openings, web pillars and barrier pillars. A correlation test of the parameters such as the width of mine opening (W_{op}), the width of web pillars and barrier pillars (W_w and W_{BP}) and the depth of hole mine opening versus the safety factor and deformation values have been carried out with a 3D model on Ansys.

The scatter test correlations show the closest relationship between W_{op} and deformation. Based on the sensitivity analysis, the most significant variable that positively affects changes in deformation is the width of the mining hole (W_{op}). At the same time, the safety factor is the variable width of the pillar (W_w) and the hole length (Lh). **Figure 9** shows a sensitivity analysis of W_{op}, W_w, W_{BP} and Lh versus the total deformation and safety factor. In contrast, the depth response to deformation does not show a significant difference. The reaction of depth change to deformation shows the shape of an S curve with minimum deformation at a depth of 136 m (0.151 m) and a maximum at a depth of 162.5 m (0.15103). It means that even if the excavation is carried out to a depth of more than 150 m as previously planned, it will not affect the deformation changes. Modelling results using the 3D Ansys model on coal Seam-C shows the safety factor < 1.3, although analytical calculations and 2D modelling using RS2 software have shown the SF value > 1.3. Therefore, for mining operations, it is necessary to strictly monitor the movement of the mine opening conditions to maintain the safety of equipment and workers.

5. Conclusions

The discussion chapter shows the stages of a comprehensive study, starting from evaluating rock stability prior to disturbance by RMR and SMR approaches followed by an analytical simulation for highwall design parameters with various dimensions of mine opening width (W_{op}), pillar width (W_w) and barrier (W_{BP}) and height (h_{op}). Next, 2D and 3D numerical modelling were carried out, and the most favourable highwall design was selected from simulation results. At the end, the depth of the highwall mining was determined from sensitivity analysis. For the case study in PT. X open-cut mine, highwall mining is feasible for seam-C and seam D, where the rock mass conditions (RMR and SMR) prior to disturbance is good. Highwall mining at the base of the slope changes the stress regime, causing deformation and possible instability. For the case of seam-C, the deformation due to highwall openings is relatively small, and the safety factor is above 1. Meanwhile, the deformation is also low for seam D, and the safety factor is higher than for seam C. Although the overall safety factor on seam-C can be considered stable, some pillars are susceptible to instability. This implies that highwall mining on seam-C needs more engineering attention, such as sequential mining and immediate backfilling. Highwall mining from seam-C and seam-D would result in a similar coal recovery of 40.54%. The stages of this research can guide highwall mining, particularly in a fairly young geologically, not-so-compacted rock in a humid tropical area with intensive weathering.

In the long term, the mining area of PT. X will continue from open pit mining to underground mining. Several preparations were started, including further exploration and topographic mapping. The preparation process requires a long time. Therefore, the highwall mining system can function as a transition activity from the surface to underground mining with low operational costs. Despite highwall mining being a transitional activity, the rock strata around the highwall mining location must be stable to ensure that the mining process runs smoothly and to guarantee the safety of workers and equipment. The stabilization of the excavation project can be obtained by comprehensively understanding the geological and geotechnical behavior around the target location and making the right geometric combination between the width of the opening hole, web pillars and barrier pillars. The safety factor must be adequate to ensure long-term stability. Regular monitoring of highwall conditions should be conducted during mining operations to assess the strength of the entry roof, pillars and highwall top surface. The right design of highwall mining can minimize the danger of highwall failure by considering disturbance factors, such as blasting vibrations, weather influences and other factors that affect the weakening of rock strength. Even with periodic geological mapping, careful geotechnical redesign and an adequate monitoring programme, the possibility of instability remains. Utilization of suitable filling materials in excavated holes can also be developed to increase the recovery of coal extraction and minimize surface subsidence.

Acknowledgement

This study was part of the research "Geotechnical study of coal mining PT.X" by the public service agency Center for Research and Development of Mineral and Coal Technology (tekMIRA), Bandung. The authors would like to thank the director of PT.X and the head of Research and Development Center for Mineral and Coal Technology for funding and data support.

6. References

Aksoy, C. O. (2008): Review of rock mass rating classification: Historical developments, applications, and restrictions. Journal of Mining Science, 44, 51–63.

Baskoro, F. R., Takahashi, K., Morikawa, K., and Nagasawa, K. (2021): System dynamics approach in determining coal utilization scenario in Indonesia. Resources Policy, 73, 102209. https://doi.org/10.1016/j.resourpol.2021.102209

Bieniawski, Z. T. (1978): "Determining rock mass deformability". International Journal of Rock Mechanics and Mining Sciences, 15, 335–343.

Bieniawski, Z. T. (1989): Engineering rock mass classifications: a complete manual for engineers and geologists in mining, civil, and petroleum engineering. Wiley-Interscience. pp. 40–47.

Bieniawski, Z.T. (1973): Engineering Classification of Jointed Rock Masses. Transactions of the South African Institution of Civil Engineers, 15, 355-344.

Bieniawski, Z.T. (1979): The Geomechanical Classification in Rock Engineering Applications. Proceedings of the 4th International Congress Rock Mechanics, Montreux, 2-8 September 1979, 41-48.

Drucker, D.C., Prager, W. (1952): Soil mechanics and plastic analysis or limit design. Quarterly of Applied Mathematics, 10(2): 157-165. http://dx.doi.org/10.1090/qam/48291.

Friederich, M. C., & van Leeuwen, T. (2017): A review of the history of coal exploration, discovery and production in Indonesia: The interplay of legal framework, coal geology and exploration strategy. International Journal of Coal Geology, 178, 56–73. https://doi.org/10.1016/j.coal.2017.04.007.

Fu, J., Haeri, H., Sarfarazi, V., Babanouri, N., Rezaei, A., Manesh, M.O., Bahrami,R., and Marji, M.F. (2023): Effects of Axial Loading Width and Immediate Roof Thickness on the Failure Mechanism of a Notched Roof in Room and Pillar Mining: Experimental Test and Numerical Simulation. Rock Mechanics and Rock Engineering, 56(1), 719–45. doi: 10.1007/s00603-022-03082-5.

Jiang, J., Lu, Y.,Wang, D., Han, X. (2022): Slope stability calculation method for highwall mining with open-cut mines. Scientific Reports, 12: 209. https://doi.org/10.1038/s41598-021-04130-w.

Jiang, J., Zhang,Z., Wang,D., Wang,L., and Han, X.(2022): Web Pillar Stability in Open-Pit Highwall Mining. International Journal of Coal Science and Technology, 9(1), 1–16. doi: 10.1007/s40789-022-00483-3.

Kundu, J., Sarkar, K., Singh, A.K., & Singh, T. (2020): Continuous functions and a computer application for rock mass rating. International Journal of Rock Mechanics and Mining Sciences, 129, 104280. https://doi.org/10.1016/j.ijrmms.2020.104280.

Kuznetsova, L.V., and Anfyorov, B.A. 2019: Combined geotechnology potentials in the process of coal deposits integrated development. IOP Conf. Series: Earth and Environmental Science 377 (2019) 012003.

Palmstrom, A. (2005): Measurements of and Correlations between Block Size and Rock Quality Designation (RQD). Tunnelling and Underground Space Technology, 20, 362-377.

Panggabean, H. (1991): Tertiary source rocks, coals and reservoir potential in the Asem Asem and Barito Basins, Southeastern Kalimantan, Indonesia, Doctor of Philosophy thesis, Department of Geology - Faculty of Science, University of Wollongong, 1991. https://ro.uow.edu.au/theses/2113

Porathur, J.L, Srikrishnan,S. Verma, C.P., Jhanwar, J. C., and Roy, P.P. (2014): Slope Stability Assessment Approach for Multiple Seams Highwall Mining Extractions. International Journal of Rock Mechanics and Mining Sciences, 70, 444–449. doi: 10.1016/j.ijrmms.2014.04.023.

Romana M. (1985): New adjustment ratings for application of Bieniawski classification to slopes. Proc. Int. Symp. on the Role of Rock Mechanics in Excavations for Mining and Civil Works, International Society of Rock Mechanics, Zacatecas, 49-53.

Ross, C., Conover,D., Baine, J. (2019): Highwall Mining of Thick, Steeply Dipping Coal–a Case Study in Geotechnical Design and Recovery Optimization. International Journal of Mining Science and Technology, 29(5),777–80. doi: 10.1016/j.ijmst.2017.12.022.

Sarfarazi, V., S. Abharian, and A. Ghorbani. (2021): Physical Test and PFC Modelling of Rock Pillar Failure Containing Two Neighboring Joints and One Hole. Smart Structures and Systems, 27(1),123–137. doi: 10.12989/sss.2021.27.1.123.

Sarfarazi, V., Fattahi,S., Asgari,K., Bahrami,R., and Wang,X. (2022): Failure Behavior of Room and Pillar with Different Room Configuration Under Uniaxial Loading Using Experimental Test and Numerical Simulation. Geotechnical and Geological Engineering,40(6),2881–2896. doi: 10.1007/s10706-022-02073-1.

Sarfarazi, V., Babanouri,N., Fattahi,S., and Asgari, K. (2023): Study on Failure Mechanism of Room and Pillar with Different Shapes and Configurations under Uniaxial Compression Using Experimental Test and Numerical Simulation. Underground Space (China), 9, 105–21. doi: 10.1016/j.undsp.2022.07.002.

Sasaoka, T., Karian, T., Hamanaka, A., Shimada, H., and Matsui, K. (2016): Application of highwall mining system in weak geological condition. International Journal of Coal Science and Technology, 3(3), 311–321. https://doi.org/10.1007/s40789-016-0121-6

Sasaoka, T., Shimada, H., Hamanaka, A., Sulistianto, B., Ichinose, M., Matsui, K. (2015): Geotechnical Issues on Application of Highwall Mining System in Indonesia. Vietrock 2015 an ISRM specialized conference (Hanoi, Vietnam)

Seib W.T. (1993): Strip mining. In: Hargraves AJ, Martin CH (eds): Australasian coal mining practice, 2nd edn. Australasian Institute of Mining Metallurgy, Carlton, pp 238–242.

Shen, B. (2014): Highwall mining stability. Proceedings of the Taishan Academic Forum – Project on Mine Disaster Prevention and Control, p. 25-37. https://doi.org/10.2991/mining-14.2014.6.

Shimada, H., Chen, Y., Hamanaka, A., Sasaoka, T., Shimada, H., Matsui, K. (2013): Application of Highwall Mining System to Recover Residual Coal in End-walls. Procedia Earth and Planetary Science, 6, 311-318. https://doi.org/10.1016/j.proeps.2013.01.041.

Sikumbang, N., and Heryanto, R. (1994): Peta Geologi Lembar Banjarmasin, Kalimantan Selatan (*Geological Map of Banjarmasin Quadrangle*), sekala 1 : 250.000 (*scale 1:250.000*). Pusat Penelitian dan Pengembangan Geologi (*Center for Geological Research and Development*), Bandung. (In Indonesian).

Small, C.A. and Morgenstern, N.R. (1992): Performance of a highwall in soft rock, Highvale mine, Alberta. Canadian Geotechnical Journal. 29(3), p. 353-363. https://doi.org/10.1139/t92-041.

SNI 03-2437- 1991 (1991): Pengujian Laboratorium Untuk Menentukan Parameter Sifat Fisik Pada Conto Batu (*Laboratory Testing To Determine Parameters Of Physical Properties In Rock Samples*), Badan Standar Nasional-BSN (in Indonesian).

SNI 2815:2011 (2011): Cara uji kuat tekan triaxial pada batu (*Method of testing triaxial compressive strength of rock*), Badan Standar Nasional-BSN (in Indonesian).

SNI 2824:2011 (2011): Cara uji geser langsung batu (*Method of testing direct shear of rock*), Badan Standar Nasional-BSN (in Indonesian).

SNI 2825:2008 (2008): Cara uji kuat tekan batu uniaksial (*Method of testing uniaxial compressive strength of rock*), Badan Standar Nasional-BSN (in Indonesian).

SNI 3406:2011 (2011): Cara uji sifat tahan lekang batu (*Method of testing slake durability of rock*), Badan Standar Nasional-BSN (in Indonesian).

Spearing, A.J.S., Zhang, J., and Ma, L. (2021): A new automated, safe, environmentally sustainable, and high extraction soft-rock underground mining method. Journal of the Southern African Institute of Mining and Metallurgy, 121(2), 89–96.

Tabaroei, A., Sarfarazi,V., Pouraminian, M., Danial, M.S. (2022): Evaluation of Behavior of a Deep Excavation by Three-Dimensional Numerical Modeling. Periodica Polytechnica Civil Engineering, 66(3), 967–77. doi: 10.3311/PPci.20353.

Tian, Y., Tu,L., Lu,X., Zhou,W., Jiskani,I.M., Liu,F., Cai,Q. (2023): Stability Analysis of Multi-Layer Highwall Mining : A Sustainable Approach for Thick-Seam Open-Pit Mines. Sustainability,15,3603. doi: 10.3390/su15043603.

Van Bemmelen, R.W. (1949): The Geology of Indonesia. IA. The Hague, Netherlands, Government. Printing Office, 732 p.

Wu, H., Chen, Y., Haoyan, L., Xie, Q., Chen,Y., and Gu, J. (2022): Stability Analysis of Rib Pillars in Highwall Mining under Dynamic and Static Loads in Open-Pit Coal Mine. International Journal of Coal Science and Technology, 9(1),38. doi: 10.1007/s40789-022-00504-1.

Van Bemmelen, R.W. (1949): The Geology of Indonesia. IA. The Hague, Netherlands, Government. Printing Office, 732 h.

Zipf, Jr., R.K. and Mark, C. (2005): Ground control for highwall mining in the United States. International Journal of Surface Mining, Reclamation and Environment, 19:3, 188-217, https://doi.org/10.1080/13895260500165353.

Zipf, R.K. (2005): Ground Control Design for Highwall Mining. Proceedings of the 2005 SME Annual Meeting (2005, Salt Lake City, UT), Society for Mining, Metallurgy & Exploration Inc. (SME), Mar 2005.

Zwillinger, D. (2014). Handbook of Differential Equations. Elsevier Science. 536 p.

SAŽETAK

Procjena stabilnosti kosina u vlažnoj tropskoj regiji: Studija slučaja rudnika ugljena u Južnom Kalimantanu, Indonezija

Kako bi unaprijedila proizvodnju, tvrtka za eksploataciju ugljena PT. X u Južnom Kalimantanu u Indoneziji, planira koristiti visokočelnu metodu iskopavanja preostalih rezervi ugljena iza završne kosine. Pri tome su glavni izazovi stabilnost i određivanje dimenzija otkopavanja zbog nepovoljnih uvjeta stijenske mase uzrokovanih intenzivnim vremenskim uvjetima i tektonikom. Cilj ovog rada je empirijskim, analitičkim i numeričkim metodama procijeniti izvedivost visokočelne metode eksploatacije u istraživanom području. Inovacija u ovom istraživanju je integracija raznih metoda, koje uključuju klasifikaciju stijenske mase, analitički proračun opterećenja i čvrstoće stijena, 2D i 3D numeričko modeliranje te procjenu dobivenog ugljena pri projektiranju visokog čela. Početno stanje je procijenjeno pomoću klasifikacije stijenske mase, a analitičkim proračunom u geometrijskom modelu utvrđene su širine iskopa i dimenzije zaštitnih stupova. Zatim je numeričkim modeliranjem ponovno procijenjena geometrija modela kako bi se dobio optimalan dizajn. Predložena je optimalna debljina i širina iskopa te raspored zaštitnih stupova od 3,20, 3,00, 3,50 odnosno 4,00 m, s četiri raspoređena stupa u jednom panelnom otkopu za sloj C te 2,50, 3,00, 3,50 i 4,00 m s četiri raspoređena stupa u jednom panelnom otkopu za sloj D. Procjena iskorištenje ugljena za sloj C i D je 40,54%. Utvrđena je međuovisnost deformacija s dimenzijama otkpnog usjeka, a faktor sigurnosti je najpromjenjiviji kod promjene dubine iskopa. Ova studija pruža preporuke za buduće eksploatacije sa visokočelnom metodom u Indoneziji i drugim regijama sa sličnim uvjetima.

Ključne riječi:
visokočelna metoda; stabilnost; empirijsko; analitičko; numeričko modeliranje

Author's contribution

Zulfahmi Zulfahmi (Ph.D. in Engineering Geology, researcher) contributed to the methodology formulation of the whole research process, data collection, analysis and literature review and was in charge of manuscript writing**. Dwi Sarah** (Ph.D. in Engineering Geology, researcher) evaluated and verified the models and corrected the manuscript writing. **Franto Novico** (Ph.D. in Engineering Geology, researcher) provided the regional and local geology analysis. **Robertus B. Susilo** (Senior Geologist, practitioner) prepared and regulated the research process and geological and geomechanical data.